Research article

Nanocomposite system with photoactive phloxine B eradicates resistant *Staphylococcus aureus*

Katarína Bilská [a], Juraj Bujdák [b,c], Helena Bujdáková [a,*]

[a] Comenius University in Bratislava, Faculty of Natural Sciences, Department of Microbiology and Virology, Ilkovičova 6, 84215, Bratislava, Slovak Republic
[b] Comenius University in Bratislava, Faculty of Natural Sciences, Department of Physical and Theoretical Chemistry, Ilkovičova 6, 84215, Bratislava, Slovak Republic
[c] Institute of Inorganic Chemistry, Slovak Academy of Sciences, Dúbravská cesta 9, 84536, Bratislava, Slovak Republic

ARTICLE INFO

ABSTRACT

Nanomaterials modified with hybrid films functionalized with photoactive compounds can be an effective system to prevent and eradicate biofilms on medical devices. The aim of this research was to extend current knowledge on nanomaterial comprised of polyurethane (PU) modified with a nanocomposite film of organoclay with the functionalized photosensitizer (PS) phloxine B (PhB). Particles of the clay mineral saponite were, at first modified by octadecyl-trimethylammonium cations to activate the surface for PhB adsorption. The colloids were filtered to get silicate films on polytetrafluoroethylene membrane filters, which were layered with a liquid mixture of PU precursors. The penetration of PU into the silicate formed a thin nanocomposite film. This nanomaterial demonstrated excellent effectiveness against methicillin-resistant *S. aureus* (MRSA) resistant to fluoroquinolones (L12 and S61, respectively). It showed more than 1000- and 10 000-fold inhibition of biofilm growth after irradiation with green laser compared to the unmodified PU material. Principal component analysis and multiple linear regression showed that the effectiveness of the nanomaterial was not influenced by virulence factors such as the expression of efflux pumps of the Nor family, the adhesin PIA encoded by the icaADBC operon or the robustness of the biofilms. However, the presence of organoclay, PhB and irradiation had a significant effect on the *anti*-biofilm properties of the nanocomposite. The antimicrobial properties of the material were strengthened after irradiation, because of high reactive oxygen species release (more than 14-fold compared to non-irradiated sample). Materials based on photoactive molecules can represent a worthwhile pathway towards the development of more complex nanomaterials applicable in various fields of medicine.

1. Introduction

Staphylococcus aureus is a member of the ESKAPE group of microorganisms that cause life-threatening infections [1,2]. Methicillin-resistant *S. aureus* (MRSA) frequently manifests not only resistance due to the expression of the *mecA* gene or beta-lactamase production, but also possesses other resistance mechanisms. The expression of efflux pumps enables it to extrude

antibacterial compounds, resulting in a significantly decreased effect of antimicrobial agents [3]. Some pumps are substrate-specific, but some of them can recognize a broad spectrum of compounds [4]. In *S. aureus*, NorA, NorB and NorC are the most important chromosomally encoded multi-drug resistant (MDR) efflux pumps, the substrates of which are fluoroquinolones (ciprofloxacin, norfloxacin), dyes (ethidium bromide, rhodamine), and quaternary ammonium compounds (tetraphenylphosphonium, benzalkonium chloride) [5–7].

Additionally, MRSA can colonize surfaces of medical devices and produce a strong biofilm surrounded by a slime matrix [8]. One of the prominent components of this extrapolymeric substance (EPS) that promotes adhesion and virulence is polysaccharide intercellular adhesin (PIA), encoded by the icaADBC operon consisting four open reading frames (*icaA, icaD, icaB,* and *icaC*) and one regulatory gene (*icaR*) [9,10].

Different approaches have been designed to prevent or reduce the biofilms formed by MRSA isolates. Small molecules, peptides, quaternized carbon dots, or coating substrates with variously modified nanoparticles have been proven to be efficient against *S. aureus* biofilms [11–14]. In general, surfaces can differ according to the antifouling mode of action that prevents the adhesion of bacteria, often in combination with a killing effect [15]. Antifouling coatings use various strategies such as the adsorption of proteins and chemically modified coatings, which leads to increased hydrophobicity of the surface, resulting in the removal of water together with microorganisms [15–17]. One of the main strategies is the release-killing and contact-killing effect of a material [18–21]. Advanced materials are usually designed to manifest a combination of several of the above-mentioned characteristics to obtain improved antimicrobial effects [22–24].

Interactions of bacteria with the surface are affected by the maturity of the biofilm and the physico-chemical properties of the respective nanomaterial, such as size, wettability, hydrophobicity, charge, and topography [25–27]. Bacterial cells interact with material through lipids, lipopolysaccharides, and surface membrane proteins [28–30]. Most bacteria primarily bind to positively charged material surfaces due to negatively charged bacterial surfaces. After the primary adhesion step, chemical forces such as van der Waals interactions are found between the outer cell wall and the material surface. Irreversible adhesion of the cells is associated with the production of EPS [31–33]. Studies showed *S. aureus* can recognize a substrate surface and position appropriate adhesins at the interface [34].

Approaches using polymeric materials with photoactive molecules seem to be highly promising [35–37]. Several studies have shown the bactericidal potential of photoactive molecules incorporated into nanoparticles, for example, nanoparticles in conjunction with boron-dipyrromethene derivates as photosensitizers (PS), carboxymethyl chitosan nanoparticles combined with methylbenzene blue (PS), or photoactive graphene quantum dots functionalized with amino group and nitrogen doping [38–40]. Hai et al. [41] investigated gold-decorated graphitic carbon nitride nanocomposites with antibacterial properties against *S. aureus* that are enhanced after illumination. These nanocomposites exhibited the photoproduction of H_2O_2 and other reactive oxygen species (ROS), which explained the mechanism of strong antibacterial activity [41]. Dadi et al. [35] focused on preparing polyurethane (PU) modified with a hybrid film based on the clay mineral saponite (Sap) functionalized with the photoactive dye phloxine B (PhB) [35,42]. The physico-chemical properties of this nanocomposite after irradiation were effective against a biofilm formed by an MRSA isolate, with a 10.000-fold reduction in growth compared to a biofilm formed on non-modified PU. It was thought that a controllable release of the active PhB significantly contributed to the antimicrobial properties of this material. During irradiation, the release of singlet oxygen and other ROS was expected, resulting in a target cell effect with a very low probability of developing resistance [43,44]. Skoura et al. [36] developed a nanocomposite layer composed of an organoclay and PhB on a polymer matrix of poly(caprolactone) that also exhibited hydrophobic, photoactive, and anti-biofilm properties against *S. aureus* [36].

Based on previous results [35,36], this study tries to answer the question of how significant are the properties of MRSA isolates, especially efflux and biofilm formation (in association with the expression of genes for the icaADBC operon) for the *anti*-biofilm activity of a nanomaterial based on Sap and photoactive PhB. Another goal was to determine whether ROS are generated during photodynamic inactivation (PDI), and whether they could contribute to the *anti*-biofilm effectiveness of the above-mentioned nanomaterial. The aim was therefore to provide further evidence of the excellent *anti*-biofilm effect of this newly-designed nanocomposite.

2. Materials and methods

2.1. Molecular identification of S. aureus and susceptibility to oxacillin, ciprofloxacin, and norfloxacin

The standard strain *S. aureus* CCM 3953 (CCM; Czech Collection of Microorganisms, Brno, Czech Republic) and 2 clinical isolates of *S. aureus* were used in this study; namely L12 and S61 were obtained from a central venous catheter and urine sample, respectively (kindly provided by prof. Lívia Slobodníková, PhD., the Institute of Microbiology, Comenius University in Bratislava, Slovak Republic). All strains were preserved in Mueller-Hinton broth (MHB, Biolife, Italy) supplemented with 60 % (v/v) glycerine (CentralChem, Slovak Republic) and stored at −20 °C. Before use, 20 μL of stock bacteria were inoculated in 50 mL of MHB and cultivated overnight on a shaker (150 rpm, Orbital Shaker-Incubator ES-20, BioSan, Latvia) at 37 °C and then plated on Mueller-Hinton agar (MHA, Biolife, Italy). Individual colonies were transferred into 100 μL of distilled water in an Eppendorf tube (Sarstedt, Germany) and heated at 100 °C for 5 min in a thermoblock (Mini Cooling Dry Bath Incubator, MC-0203, Major Science, USA). Then, samples were immediately placed on ice and after 3 min, tubes were centrifuged at 6000×*g* (High-Speed Microliter Centrifuge Frontier TM 5515R, Ohaus Europe GmbH, Switzerland) for 5 min. Fifty μL of these samples were pipetted into a new Eppendorf tube and used directly for PCR.

Assignment to the *S. aureus* species was confirmed using PCR with primers specific for the *femA* gene, and the presence of the *mecA* gene was determined by PCR according to Braoios et al. [45]. Primers and conditions for PCR are summarized in Supplementary data.

Susceptibility to oxacillin, ciprofloxacin, and norfloxacin (Liofilchem®, Italy) was tested using E-tests according to the European

Committee on Antimicrobial Susceptibility Testing (EUCAST) protocol (version 2023) [46]. Susceptibility to oxacillin and ciprofloxacin was evaluated according to the EUCAST protocol, and to norfloxacin according to the Clinical and Laboratory Standards Institute (CLSI) [47], since EUCAST does not determine breakpoint criteria.

2.2. Biofilm and slime production assays

For biofilm preparation, overnight cultures prepared in MHB (37 °C, 18 h) were inoculated in MHB supplemented with 4 % (w/v) glucose ($OD_{600} = 0.05$; Visible Spectrophotometer S-220 UV, Boeco, Germany) and incubated at 37 °C on a shaker (150 rpm) until the exponential phase ($\approx$2.5 h; $OD_{600} = 0.5$). Then, 100 μL of suspension was inoculated in 96-well microtiter plates (Sarstedt, Germany). Wells were filled with 100 μL of fresh MHB +4 % glucose (CentralChem, Slovak Republic). The plates were incubated statically at 37 °C for 24 h to develop a biofilm. The biofilm was evaluated by crystal violet assay according to Merrit et al. [48], but slightly modified [49]. The results were expressed according to the criteria of Stepanović et al. [50].

Biofilm and slime production was also tested by the Congo Red Agar (CRA) method [51]. Briefly, CRA was prepared as Brain Heart Infusion (BHI, BioLife, Italy) agar supplemented with Congo Red (0.08 %; w/v; Erba Lachema, Czech Republic), sucrose (5 %; w/v; Sigma-Aldrich, Germany), glucose (2 %; w/v), NaCl (1.5 %; w/v; CentralChem, Slovak Republic), and vancomycin (0.5 mg/mL, Sigma-Aldrich, Germany). The prepared overnight cultures were diluted to a density corresponding to 0.5 McFarland Standard (1.5×10^5 bacteria/mL) in 1xPBS. The Petri dish with CRA was divided into sectors and inoculated with 5 μL of appropriate suspension. The CRA plates were cultivated at 37 °C. After 24 h, biofilm and slime production were assessed by the colour of the colonies: black/dark red colour represented strong producers; red/light red colonies represented weak producers.

2.3. Evaluation of efflux activity in vitro

Efflux activity was performed by the ethidium bromide (EtBr) agar screening method [3] with minor modifications. Briefly, Petri dishes with Tryptic Soy Agar (TSA; Condalab, Spain) supplemented with different concentrations of EtBr (1; 1.5; 2; and 2.5 μg/mL, Serva, Germany) were used for testing. Overnight cultures of *S. aureus* adjusted to 0.5 McFarland standard in 1xPBS were inoculated on TSA plates and cultivated in the dark (24 h, at 37 °C). Plates were then examined under a UV-Transilluminator (MUV 21-312-220, Major Science, USA) at λ 254 nm. Strains were evaluated according to fluorescence signal strength, which correlated with the activity of efflux pumps (no fluorescence when a strain manifested high efflux activity, and fluorescence was observed when the strain was less active, or no efflux activity was present). Clinical isolates of L12 and 61 were compared to the standard strain *S. aureus* CCM without efflux activity.

2.4. Isolation of RNA and qPCR analysis of genes coding for the IcaA and IcaD membrane proteins, and efflux pumps from the Mdr family

RNA was isolated from the suspension of bacteria prepared in an exponential phase as described previously. Phenol/chloroform extraction was used to isolate the RNA. Briefly; the mixture containing 700 μL of phenol/chloroform (5:1; phenol from AppliChem, Germany, chloroform from CentralChem, Slovak Republic), 700 μL of AE buffer (0.5 M EDTA, 3 M CH_3COONa, CH_3COONa all from Sigma-Aldrich, Germany) and 66 μL of 20 % (w/v) SDS (AppliChem, Germany) was prepared for lysis and preheated at 65 °C for 30 min. Bacterial suspensions were centrifuged at $6000 \times g$ for 5 min, and pellets were mixed with the phenol/chloroform solution. The samples were incubated at 65 °C for 30 min and then placed on ice for 5 min. The samples were then centrifuged at $14\,000 \times g$ for 5 min at 4 °C. The supernatant was transferred into a new Eppendorf tube, mixed with phenol/chloroform solution in a 1:1 ratio, and vortexed. Centrifugation was repeated, and the supernatant was mixed with chloroform:isoamyl alcohol (24:1, Sigma-Aldrich, Germany) in a 1:1 ratio and vortexed. After the next centrifugation, 300 μL of the supernatant was added to 600 μL of 96 % ethanol (CentralChem, Slovak Republic) and 30 μL of 3 M CH3COONa. The samples were kept overnight at −80 °C. The next day, the samples were centrifuged at $16\,000 \times g$ for 20 min at 4 °C, and the supernatant was discarded. A volume of 500 μL of 70 % (v/v) ethanol was added to an Eppendorf tube and mixed. Samples were then centrifuged at $16\,000 \times g$ for 15 min at 4 °C. The supernatant was discarded,

Table 1
List of oligonucleotide sequences used in this study.

Gene		Sequence 5′- 3′	Amplicon size	Reference
icaA	Forward	TTT CGG GTG TCT TCA CTC TAT	229 bp	Shang et al. [54]
	Reverse	CGT AGT AAT ACT TCG TGT CCC		
icaD	Forward	CCA GAC AGA GGG AAT ACC	82 bp	
	Reverse	AAG ACA CAA GAT ATA GCG ATA AG		
norA	Forward	ATC GGT TTA GTA ATA CCA GTC TTG C	120 bp	Kong et al. [55]
	Reverse	GCG ATA TAA TCA TTT GAG ATA ACG C		
norB	Forward	ATG GAA AAG CCG TCA AGA GA	110 bp	
	Reverse	AAC CAA TGA TTG TGC AAA TAG C		
norC	Forward	ATG AAT GAA ACG TAT CGC GG	120 bp	
	Reverse	GTC TGC ACC AAA ACT TTG TTG TAA A		
rpoD	Forward	CAC GAG TGA TTG CTT GTC	146 bp	Theis et al. [53]
	Reverse	GAT ACG TAG GTC GTG GTA TG		

and the pellet was dried at room temperature (RT). Finally, a volume of 30 μL of Nuclease-free water was added. The RNA concentration was measured using NanoDrop Spectrophotometer, ND-1000 (NanoDrop Technologies, USA) and stored at −80 °C until used. Before qPCR, RNA of samples was treated with DNase I, RNase-free (Thermo Scientific, USA), and cDNA was synthesized using a Maxima First Strand cDNA Synthesis kit for RT-qPCR (Thermo Scientific, USA) according to the manufacturer's instructions; cDNA samples were stored at −20 °C until used.

In real-time quantitative PCR (qPCR), sets of primers listed in Table 1 were used. All primers were synthetized by Metabion International AG Planegg/Steinkirchen, Germany. A thermal protocol for qPCR was established according to the manufacturer's instructions. The annealing temperature was set to 55 °C for 20 s. HOT FIREPol® EvaGreen® qPCR Mix Plus (Solis BioDyne OÜ, Tartu, Estonia) and a Mx3000P qPCR system (Agilent Technologies, Inc., Santa Clara CA, USA) were used for qPCR. Data were analyzed using Agilent Technologies' MxPro software. Relative gene expression was calculated using the $2^{\Delta\Delta CT}$ method [52]. The *rpoD* housekeeping gene was used as the control [53]. Values for strain *S. aureus* CCM were set as the controls and normalized to 1.

2.5. Anti-biofilm activity of PU modified with nanocomposites functionalized with Sap and PhB

Anti-biofilm effectiveness was tested on PU (VARNISH-PU 2 KW, Isomat S.A., Thessaloniki, Greece) with a hybrid film, the preparation of which has already been detailed described by Dadi et al. [35]. Briefly, colloidal dispersion of Sap (Sumecton, Kunimine Ind., Tokyo, Japan) and solutions of octadecyltrimethylammonium (ODTMA, Sigma-Aldrich, Germany) cations and PhB (Sigma-Aldrich, Germany) were prepared in deionized water. Sap dispersion was mixed with ODTMA or ODTMA and PhB solutions to get $n_{ODTMA}/m_{Sap} = 0.8$ mmol/g and $n_{PhB}/m_{Sap} = 0.05$ mmol/g. The mixtures were shaken at 40 °C at 150 rpm for 24 h. The colloids were filtered through 0.1 μm polytetrafluoroethylene membrane filters (Omnipore™, Millipore, Merck, Germany) by vacuum filtration. Thin silicate films deposited on membranes were covered with a mixture of liquid PU precursors and let to cure at RT for about 24-h. PU pellets with thin composite films were peeled off the membranes. For each strain, PU alone, PU with nanocomposite film based on Sap modified with ODTMA (PUC) and PUC functionalized with PhB (PUC + PhB) were tested. A sample of PUC + PhB was irradiated with a green laser for 2 min (5 cm from the surface of PU; $\lambda = 532$ nm, 100 mW, Alligator, MZTech s.r.o., Košice, Slovak Republic). *Anti*-biofilm effectiveness was tested according to the protocol of Dadi et al. [35], and evaluated by the calculation of colony-forming units (CFU). Each sample was prepared in at least 3 parallels, and the experiment was repeated 3 times. Results represent average values with standard deviations. The growth of bacteria on PU alone was set as a control.

2.6. Measurement of ROS production

The Production of ROS was measured using a ROS-Glo™ H_2O_2 Assay kit (Promega, USA) with minor modifications. Briefly, the biofilm was prepared as described. Eighty μL of biofilm cells were added to a white polystyrene 96-well plate (Greiner Bio-One, Germany), 100 μM menadione (Sigma-Aldrich, Germany) was used as a positive control, and distilled water was used as a negative control. The stock solution of menadione was prepared fresh in acetone (CentralChem, Slovak Republic) before each experiment, then the 100 μM menadione was prepared in distilled water. Then according to the provider's protocol, H_2O_2 substrate (20 μL) and 100 μL of Ros-Glo™ Detection Solution were pipetted into wells followed by a 20-min incubation in the dark at RT. Afterwards, luminescence was measured with a GloMax® Discover (Promega, USA). The results were expressed in relative luminescence units (RLU) representing ROS production. The final values represent an average of RLU with standard deviation calculated from 3 independent experiments, with 3 parallel samples in each of them.

2.7. Statistical analysis

Statistical significance was determined with the two-tailed Student's t-test using the software GraphPad Prism (Graph Pad, San Diego CA, USA). $p < 0.05$ (*) was considered statistically significant; $p < 0.01$ (**); $p < 0.001$ (***); $p < 0.0001$ (****).

Principal component analysis (PCA) and multiple linear regression (MLR) were applied to analyse the data of respective *S. aureus* strains, including their ability to form a biofilm, gene expression, *anti*-biofilm effectiveness related to various materials, and sample's irradiation. Therefore, the assumed factors were as follows: the identities of respective *S. aureus* strains (CCM, L12, S61); biofilm formation; expression of the *norA*, *norB*, *norC*, *icaA*, and *icaD* genes; biofilm inhibition on various materials (organoclay or organoclay modified with PhB), and irradiated samples. All the variables were normalized to maxima in a respective series of values. The identity of microorganisms, the presence of materials' components or experiments with irradiation were converted to numeric indices of either 1 or 0 before the analyses. PCA was analyzed using The Unscrambler® 10.3. Software (Camo, Norway). MLR was used to verify the results of PCA on the same set of data applying a multi-linear model by combining predictor variables in linear combinations of the factors to express the inhibition of the biofilm as a dependent variable. More information on the methods has been published elsewhere [56].

3. Results

3.1. Characterization of S. aureus strains: resistance, biofilm formation, and expression of the icaA and icaD genes

All bacterial strains were confirmed to be *S. aureus* species, as the *femA* gene was detected by PCR (Supplementary data, Fig. S1). The *mecA* gene was found in isolates of S61 and L12, confirming the methicillin-resistance genotype. The standard strain *S. aureus* CCM

did not possess the *mecA* gene (Supplementary data, Fig. S1). Results from E-tests confirmed an oxacillin-resistance phenotype of strains of S61 and L12 (both with MIC >256 μg/mL), while the standard strain was oxacillin-sensitive (MIC = 0.25 μg/mL). Results are summarized in Fig. 1. Additionally, isolates of S61 and L12 exhibited resistance against tested fluoroquinolones, while the standard strain was sensitive (Fig. 1A.)

Biofilm and slime production evaluated by CV staining (Supplementary data Fig. S2) and the CRA method agreed and confirmed that the standard strain CCM and isolate S61 were strong biofilm and slime producers, while L12 was rated as a moderate producer (Fig. 1A and B).

PCR confirmed the presence of the *icaA* and *icaD* in every tested strain (Supplementary data, Fig. S3). The results from qPCR showed that the native expression of both *icaA* and *icaD* genes was slightly increased in the S61 isolate, while upregulation in L12 was not relevant (it was below 2-fold up-regulation) compared to standard strain CCM, set as 1 (Fig. 2).

3.2. Efflux activity of S. aureus strains

The ability to expel compounds from cells by efflux was evaluated by the ethidium bromide agar screening method (Fig. 3A and B). Fig. 3 A shows the growth of all strains on TSA without EtBr, and Fig. 3B demonstrates the different efflux activity of tested strains, with the highest efflux found in S61 (black colour - low fluorescence signal) and lower in the L12 isolate (weaker white colour - decreased fluorescence signal). The standard strain did not exhibit efflux activity (white colour – high fluorescence signal). These results agreed with qPCR determining the native expression of the *norA, norB* and *norC* genes associated with quinolone resistance (Fig. 3C). The results showed a significantly higher expression of the *norA* gene for S61 and L12 isolates compared to the standard strain CCM. Increased expression of the *norB* and *norC* genes were not examined in the tested strains.

3.3. Evaluation of anti-biofilm effectiveness of PU modified with hybrid films

The *anti*-biofilm effectiveness of PU modified with hybrid films based on saponite and PhB (Fig. 4) showed a significant inhibition of biofilm growth compared to PU alone. Moreover, the effect was significantly increased after irradiation. The PUC + PhB samples in the dark exhibited a more than 100-fold growth reduction for each strain compared to their control biofilm formed on PU alone. After the irradiation of PUC + PhB, the reduction was even up to 10 000- and 1000-fold higher (from around 10^8 cells/mL to around 10^4-10^5 cells/mL) for strains of CCM and S61 and L12 strain, respectively, compared to their control biofilms on PU alone.

3.4. Analysis of the influence of biofilm formation and gene expression on the anti-biofilm effectiveness of hybrid material

PCA was used to estimate the relationship between individual variables and to characterize the complexity of the system related to the number of principal components (Fig. 5A–C). Although the method as such does not distinguish between dependent and independent variables, the aim was to find relationships between various factors, in particular the inhibition of biofilm growth. The factors to be analyzed included the identity of microorganisms, gene expression, ability to form a biofilm, input data of antimicrobial tests or the tested materials, and the resulting suppression of biofilm formation. The parameter of explained variance indicates the proportion to which the mathematical model describes the analyzed data. The number of PCs needed to achieve an above 95 % explained variance of the analyzed data was five. With the number of principal components in the PC1-PC5 series, the explained variance values (in %) were 32, 61, 86, 93 and 98. The contribution of the first three components was the most significant (each with an explained variance value above 20 %). The impact of PC4 and PC5 were lower and contributed to the explained variance by 7 % and 4.5 %, respectively.

Loadings as a result of PCA analysis shown in Fig. 5A–C describe how much each variable contributes to a particular principal component. PC1, responsible for the highest variance of the data, describes particularly well the differences between microorganisms, and partially their relationship to other factors. CCM achieves a positive loading value, S61 a negative one, and L12 a less significant negative value. The biggest difference was between CCM and S61, and L12 exhibits properties between these microorganisms. Loading for S61 correlates well with a similar value for the *norA* gene expression, less but still significantly with the *icaA* and *icaD* genes. This means that these parameters are especially important for the S61 microorganism. The other parameters are close to zero, which can be
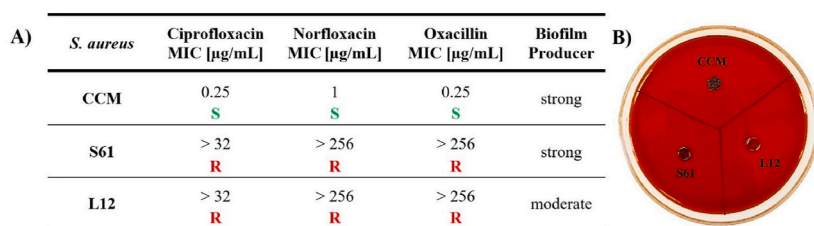

A)	*S. aureus*	Ciprofloxacin MIC [μg/mL]	Norfloxacin MIC [μg/mL]	Oxacillin MIC [μg/mL]	Biofilm Producer
	CCM	0.25 S	1 S	0.25 S	strong
	S61	> 32 R	> 256 R	> 256 R	strong
	L12	> 32 R	> 256 R	> 256 R	moderate

Fig. 1. A) Antimicrobial susceptibility profiles for oxacillin and fluoroquinolones (ciprofloxacin and norfloxacin), evaluation of biofilm formation of *S. aureus* strains. **S** represents sensitive phenotype strains; R represents resistant phenotype strains; **B)** CRA method for testing biofilm and slime production. Black/dark red colonies represent strong biofilm and slime producers; light red colonies represent weak biofilm producers. (For interpretation of the references to colour in this figure legend, the reader is referred to the Web version of this article.)
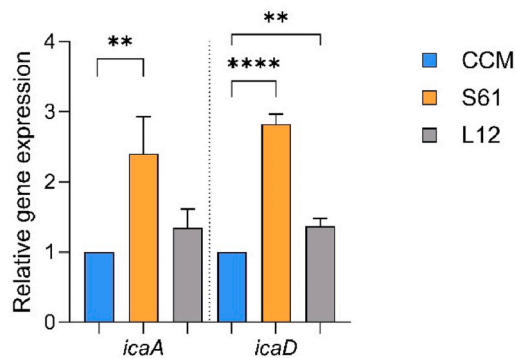
Fig. 2. Relative changes in expression of *icaA* and *icaD* genes in planktonic cells of *S. aureus* S61 and L12 compared to standard strain *S. aureus* CCM 3953, set as 1; *rpoD* was used as the housekeeping gene. A $p < 0.01$ (**) was considered very significant; $p < 0.001$ (***) and $p < 0.0001$ (****) extremely significant.
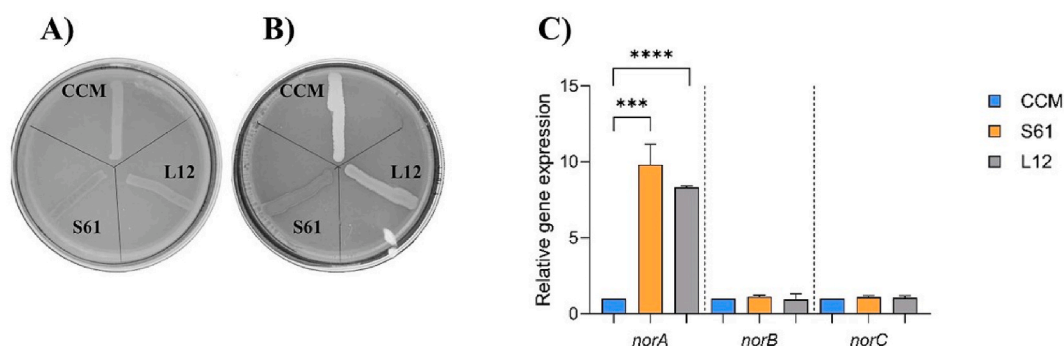

Fig. 3. Assessment of efflux activity by EtBr screening method: **A)** control TSA without EtBr; **B)** TSA supplemented with 1 μg/mL of EtBr; **C)** relative changes in expression of the *norA, norB* and *norC* efflux genes in planktonic cells S61 and L12 compared to strain CCM of corresponding genes, set as 1; *rpoD* was used as the housekeeping gene. A $p < 0.001$ (***) was considered highly significant and $p < 0.0001$ (****) extremely significant.
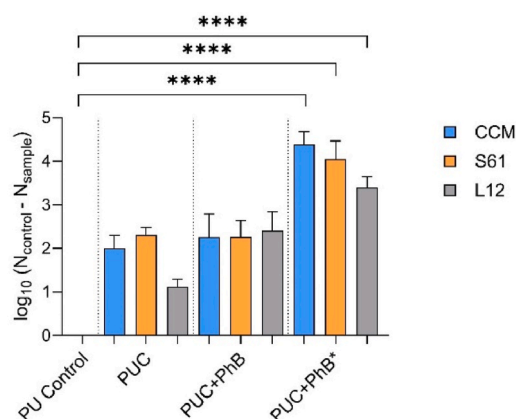

Fig. 4. *Anti*-biofilm effectiveness of PU with hybrid films based on saponite and PhB expressed as the decadic logarithm of biofilm cell reduction. The function $\log_{10} (N_{control}/N_{sample})$; $N_{control}$ represents the number of biofilm cells/mL on non-modified PU material; N_{sample} represents the number of biofilm cells/mL on modified PU material (PUC, PUC + PhB); *represents samples irradiated with a green laser. A $p < 0.0001$ (****) was considered extremely significant. (For interpretation of the references to colour in this figure legend, the reader is referred to the Web version of this article.)

interpreted as not being related to the type of microorganism.

PC2 was the second most significant component. Non-zero loading was described mainly by the presence of organoclay, PhB, and the effect of irradiation on the inhibition of biofilm growth. The influence of the type of microorganism or the activation of genes or
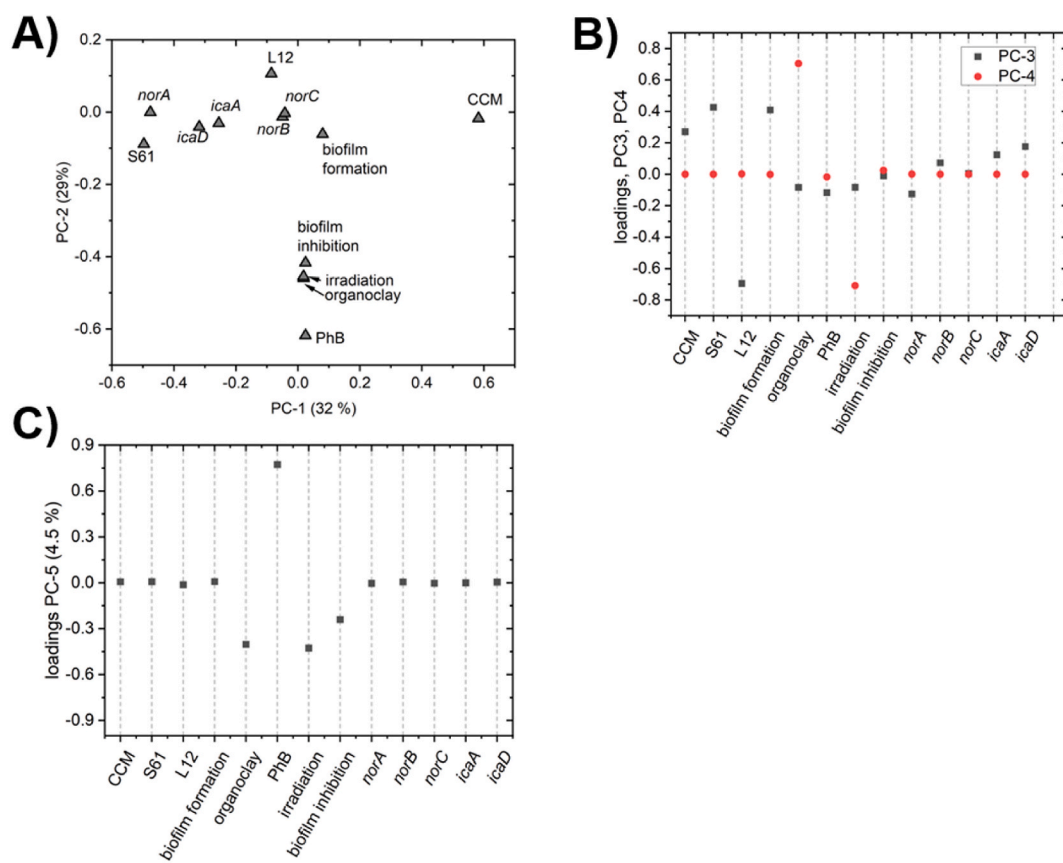
Fig. 5. A) PCA loading plot showing the relation between the first two components; **B)** Loadings of factors for principal components PC3 and PC4; **C)** Loadings of factors for principal components PC3 and PC4; Efflux genes: *norA*, *norB*, *norC*; ica genes: *icaA, icaD*; PhB – phloxine B.

other characteristics of microorganisms was not demonstrated. The values of the loadings of these parameters were close to zero or exhibited smaller loadings, which can be interpreted as a small or insignificant effect. It seems that S61 exhibits a slightly higher tendency for biofilm inhibition than L12. The PCA loadings plot showing the dependence between PC1 and PC2 shows the association between the individual factors based on the distances between the points in the graph. It should be noted that PC1 and PC2 still only represent around 60 % of the variance. In addition, the previously noted association of *norA* formation with microorganism S61 was observed.

PC3 represents up to 25 % of the variance, but most variables are close to zero (Fig. 5A). Biofilm formation, expressing the different tendencies of microorganisms to form a biofilm, gave a highly positive value. A similar value for S61 confirmed the increased ability of this microorganism to form biofilms. A partially increased value was also observed for strain CCM, but the opposite trend was observed for the L12 isolate. The indication of a weak correlation with other parameters such as the *icaA* and *icaD* gene expression is not significant. PC4 explains significantly less variance than the previous PC1-PC3. Only two variables have non-zero loading values in their inverse correlation. These variables relate to the setup of the tests for biofilm inhibition, and do not include dependent variables.

In contrast, interesting results were provided by PC5 (Fig. 5C), even though it contributed to only a very small explained variance. By including PC5, the explained variance increased from 93.3 to 97.8 %, which is less than a 5 % change. Non-zero loading of biofilm inhibition was manifested here for the second time. It had a negative value, being in direct correlation with the presence of organoclay and irradiation. PhB as a variable had an inverse correlation with biofilm inhibition. The factor of biofilm inhibition was already observed for PC2 (Fig. 5A), and the correlation between biofilm inhibition and the presence of PhB was the highest. PC5 can be interpreted as showing that PhB alone without irradiation and neglecting the organoclay effect has a smaller influence on biofilm inhibition than the same material when irradiated (Fig. 5C). However, the most important result related to PC5 is the non-significant influence of the other variables, and their loadings were very close to zero.

The effect of variables on biofilm inhibition was verified by another method, MLR. Similar to the PCA analysis (see PC5), the MLR method did not find any significant correlation between biofilm inhibition and the respective microorganisms, nor with their ability to form a biofilm or gene expression. Only the presence of organoclay, PhB, and irradiation exhibited a dominant influence. The MLR calculation was repeated after reducing predictor variables to the significant ones (Table 2) and a relatively high $R^2 = 0.97$ was achieved. The positive correlation with these factors is semi-quantitatively expressed using β parameters. Statistically, the significance of the influence of the factors is expressed using t- and P-values, for which the threshold of significance is at $t > 2$ and $P < 0.05$,

respectively. From the standard errors of β coefficients and t- and P-values, a less convincing influence of the PhB parameter can be inferred. The reason for this may be the fact that no tests were done with irradiated samples with organoclay but without PhB. Therefore, the effects of the presence of PhB and irradiation should be interpreted together. The effects of some other variables were verified by a series of additional MLR calculations, in which a fourth independent variable was added. For all combinations, again all other factors came out as insignificant. The factor of biofilm formation ability came closest to the significance threshold when included in the calculation: (t-value $= 1.7$, P-value $= 0.10$, $\beta = 0.05 \pm 0.03$). Its influence may exist but is overwhelmed by three very significant factors: the presence of organoclay, PhB, and irradiation.

3.5. Production of ROS on hybrid photoactive PU material

The production of ROS was measured on non-modified and modified PU. The amount of ROS expressed by RLU was not significantly increased on PUC and PUC + PhB without irradiation compared to PU alone. However, after irradiation, ROS were immediately generated, manifesting a 25-fold increase in RLU for standard strain CCM and 14-fold for both clinical isolates of L12 and S61. Results are summarized in Fig. 6.

4. Discussion

MRSA isolates represent an immense challenge for medicine, as these bacteria harbour various resistance mechanisms and virulence factors [2,57]. For example, the administration of fluoroquinolone to patients can lead to a dual effect; it promotes increased adherence and favours MRSA colonization over susceptible *S. aureus* [57,58].

Moreover, the formation of biofilms on medical devices complicates the treatment of bacterial infections [1,59]. Therefore, the search for new materials with antimicrobial properties is a significant part of current research. The most desirable are those nanomaterials which combine several mechanisms of action against microorganisms [35,36]. Nanomaterials with photoactive properties for medical use represent a relatively new group of materials. Qu et al. [60] confirmed the excellent synergic effect of a polydopamine layer with a phase-transited bovine serum albumin film with antifouling activity, while the effectiveness of the material against *S. aureus* was improved by the photothermal effect of the layer after near-infrared irradiation [60]. Another study conducted by Wang et al. [61] developed superhydrophobic and photodynamic bactericidal membranes functionalized with the photosensitizer Chlorin e6, and reported antifouling activity and the generation of ROS after irradiation with visible light. The tested membranes exhibited high physical stability and bactericidal activities against both Gram-positive and Gram-negative bacteria [61].

It has already been mentioned that this work is a continuation of the research of Dadi et al. [35], and provides further insight into the effectiveness of the previously mentioned modified PU on MRSA isolates, with a focus on their efflux activity and biofilm production in association with the activity of genes coding for the icaADBC operon. Additionally, the formation of ROS was monitored during PDI of biofilm on a modified PU nanocomposite. For this study, a standard strain and two MRSA isolates were selected. Clinical isolates were also resistant to ciprofloxacin and norfloxacin. Results from the EtBr screening method and qPCR proved that both isolates manifested effective efflux activity mediated by the *norA* gene. The results of our study are in accordance with Pourmehdi et al. [62] which confirmed the presence of the NorA efflux pump in *S. aureus* strains resistant to ciprofloxacin [62]. However, PCA analysis did not prove any correlation with the antimicrobial activity of modified PU, even after irradiation. This is important information, as this type of pump could participate in the efflux of drugs and other compounds including PS, as has been previously described for methylene blue [63,64]. Based on the above observations, it can be noted that the expression of the efflux transporters from an MFS class does not play any role in influencing the *anti*-biofilm effectiveness of PhB.

The ability to form a biofilm is an important virulence factor of pathogenic microorganisms. While standard strain and MRSA isolate S61 proved to be strong biofilm and slime producers, isolate L12 was a weak producer. The formation of a biofilm is strongly associated with PIA adhesin, with the *icaA* and *icaD* genes playing a crucial role [65,66]. PIA is a cationic exopolysaccharide, which is an important component of the extracellular matrix and contributes to biofilm formation in both *S. aureus* and *S. epidermidis* [10,67]. It has been reported that PIA plays a key role in the surface hydrophobicity of *S. epidermidis*, and mediates initial adherence steps. Positively charged PIA bonds to the negatively charged wall teichoic acids and increases resistance to mechanical force and flow conditions such as those found in catheters [10,68]. The tested strains exhibited different regulation of both genes, with the highest observed expression for the MRSA strain S61. However, neither PCA nor MLR analysis confirmed any correlation between changes in the *icaA* and *icaD* gene expression and inhibition of biofilm growth on the material.

PU materials modified with photoactive hybrid films were prepared for testing *anti*-biofilm properties according to Dadi et al. [35]. The composite of PUC + PhB without irradiation exhibited a more than 100-fold reduction in the survival of resistant strains (L12 and S61), suggesting that a surface with PhB [35,36] is an important parameter for antimicrobial effectiveness, which was also confirmed by PCA. Additionally, the irradiation of PUC + PhB increased this reduction to 1000 and 10 000-fold for L12 and S61, respectively, compared to non-modified PU. A significant contribution of irradiation was also supported by PCA. Moreover PCA, in agreement with MLR analysis, showed that the effectiveness of the photoactive nanocomposite PUC + PhB on the tested strains can be correlated with the functionality of an organoclay modified with PhB and irradiated, while biofilm properties and the resistance of MRSA isolates did not demonstrate any impact on the *anti*-biofilm activity of the PUC + PhB nanocomposite.

Photoactive compounds are known for generating ROS after irradiation, which damage bacterial cells [43,44]. Generally, the measurement of ROS can be done by determining generated H_2O_2 [69,70]. The production of H_2O_2 on non-modified and modified PU material was compared before and after irradiation. The results confirmed a more than 14-fold increase in RLU immediately after irradiation for all strains compared to samples formed on non-modified PU. These results are supported by the observations of Qi et al.

Table 2

Results of multi-linear regression with biofilm inhibition as dependent variable and significant predictor variables.

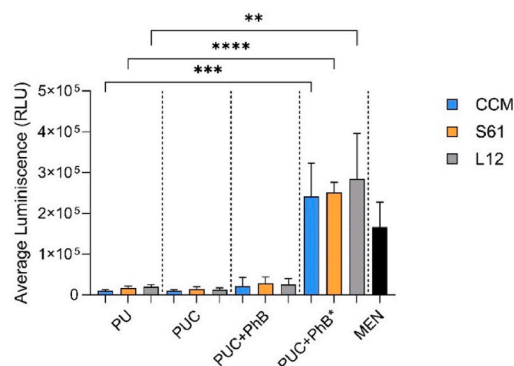| Factors/independent variables	β	t-value	p-value
Organoclay	0.39 ± 0.03	12.7	10^{-14}
phloxine B	0.11 ± 0.04	2.4	0.02
Irradiation	0.35 ± 0.04	8.1	10^{-9}

Fig. 6. ROS production expressed in RLU before and after irradiation of PU alone and PU modified with hybrid film. MEN represents a solution of menadione (100 μM) as the positive control. A $p < 0.01$ (**) was considered very significant; $p < 0.001$ (***) highly significant, and $p < 0.0001$ (****) extremely significant. *Samples irradiated with green laser. (For interpretation of the references to colour in this figure legend, the reader is referred to the Web version of this article.)

[69], who showed that the photodynamic activation of PhB resulted in significant H_2O_2 release, which suggested that PhB induces the photodynamic effect through an H_2O_2-dependent mechanism [36,69]. Moreover, other properties of the strains studied in this work did not show an important difference in terms of ROS production.

5. Conclusions

The results of this work significantly extended current knowledge on nanomaterials comprised of PU modified with a nano-composite film of organoclay with the functionalized photoactive molecule PhB. This nanomaterial demonstrated excellent effectiveness against MRSA strains. PCA and MLR analysis suggested that the efficacy was not affected by the expression of MFS-type efflux transporters, nor the ability to form a robust biofilm. This is an important finding, indicating that the material is effective against *S. aureus* strains regardless of their resistance or manifested virulence factors. Additionally, the antimicrobial properties of the material were strengthened after irradiation, because of high ROS release. Materials based on photoactive molecules can represent a worthwhile pathway towards the development of more complex nanomaterials applicable in various fields of medicine.

Data availability

Data will be made available on request.

CRediT authorship contribution statement

Katarína Bilská: Writing – review & editing, Writing – original draft, Methodology, Investigation, Conceptualization. **Juraj Bujdák:** Writing – review & editing, Writing – original draft, Software, Methodology, Conceptualization, Funding acquisition. **Helena Bujdáková:** Writing – review & editing, Writing – original draft, Validation, Supervision, Project administration, Funding acquisition, Conceptualization.

Declaration of competing interest

Authors declare that they have no known competing financial interests or personal relationships that could have appeared to influence the work reported in this paper.

Acknowledgements

Appendix A. Supplementary data

Supplementary data to this article can be found online at https://doi.org/10.1016/j.heliyon.2024.e33660.

References

[1] N.C.T. Dadi, B. Radochová, J. Vargová, H. Bujdáková, Impact of Healthcare-associated infections connected to medical devices—an update, Microorganisms 9 (2021) 2332, https://doi.org/10.3390/microorganisms9112332.

[2] M. Shoaib, A.I. Aqib, I. Muzammil, N. Majeed, Z.A. Bhutta, M.F.-A. Kulyar, M. Fatima, C.-N.F. Zaheer, A. Muneer, M. Murtaza, M. Kashif, F. Shafqat, W. Pu, MRSA compendium of epidemiology, transmission, pathophysiology, treatment, and prevention within one health framework, Front. Microbiol. 13 (2023) 1067284, https://doi.org/10.3389/fmicb.2022.1067284.

[3] B.P. Howden, S.G. Giulieri, T. Wong Fok Lung, S.L. Baines, L.K. Sharkey, J.Y.H. Lee, A. Hachani, I.R. Monk, T.P. Stinear, Staphylococcus aureus host interactions and adaptation, Nat. Rev. Microbiol. (2023) 1–16, https://doi.org/10.1038/s41579-023-00852-y.

[4] A. Dashtbani-Roozbehani, M.H. Brown, Efflux pump mediated antimicrobial resistance by staphylococci in health-related environments: challenges and the quest for inhibition, Antibiotics 10 (2021) 1502, https://doi.org/10.3390/antibiotics10121502.

[5] S. Costa, E. Junqueira, C. Palma, M. Viveiros, J. Melo-Cristino, L. Amaral, I. Couto, Resistance to antimicrobials mediated by efflux pumps in Staphylococcus aureus, Antibiotics 2 (2013) 83–99, https://doi.org/10.3390/antibiotics2010083.

[6] S.S. Costa, B. Sobkowiak, R. Parreira, J.D. Edgeworth, M. Viveiros, T.G. Clark, I. Couto, Genetic diversity of norA, coding for a main efflux pump of Staphylococcus aureus, Front. Genet. 9 (2019) 710, https://doi.org/10.3389/fgene.2018.00710.

[7] S.G. Solano-Gálvez, M.F. Valencia-Segrove, M.J.O. Prado, A.B.L. Boucieguez, D.A. Álvarez-Hernández, R. Vázquez-López, S.G. Solano-Gálvez, M.F. Valencia-Segrove, M.J.O. Prado, A.B.L. Boucieguez, D.A. Álvarez-Hernández, R. Vázquez-López, Mechanisms of resistance to quinolones, in: Antimicrob. Resist. - One Health Perspect., IntechOpen, 2020, https://doi.org/10.5772/intechopen.92577.

[8] F.F. Tuon, P.H. Suss, J.P. Telles, L.R. Dantas, N.H. Borges, V.S.T. Ribeiro, Antimicrobial treatment of Staphylococcus aureus biofilms, Antibiotics 12 (2023) 87, https://doi.org/10.3390/antibiotics12010087.

[9] S.E. Cramton, C. Gerke, N.F. Schnell, W.W. Nichols, F. Götz, The intercellular adhesion (ica) locus is present in Staphylococcus aureus and is required for biofilm formation, Infect. Immun. 67 (1999) 5427–5433.

[10] H.T.T. Nguyen, T.H. Nguyen, M. Otto, The staphylococcal exopolysaccharide PIA – biosynthesis and role in biofilm formation, colonization, and infection, Comput. Struct. Biotechnol. J. 18 (2020) 3324–3334, https://doi.org/10.1016/j.csbj.2020.10.027.

[11] J. Zhang, L. Shen, P. Zhou, S. Chen, B. Wang, C. Wan, W. Han, L. Rao, H. Zhao, X. Wang, C. Wu, J. Shi, Y. Xiao, Z. Song, F. Yu, C. Lin, A novel small-molecule compound S-342-3 effectively inhibits the biofilm formation of Staphylococcus aureus, Microbiol. Spectr. (2023) e0159623, https://doi.org/10.1128/spectrum.01596-23.

[12] L. Rao, Y. Sheng, J. Zhang, Y. Xu, J. Yu, B. Wang, H. Zhao, X. Wang, Y. Guo, X. Wu, Z. Song, F. Yu, L. Zhan, Small-molecule compound SYG-180-2-2 to effectively prevent the biofilm formation of methicillin-resistant Staphylococcus aureus, Front. Microbiol. 12 (2022) 770657, https://doi.org/10.3389/fmicb.2021.770657.

[13] H.-H. Ran, X. Cheng, Y.-W. Bao, X.-W. Hua, G. Gao, X. Zhang, Y.-W. Jiang, Y.-X. Zhu, F.-G. Wu, Multifunctional quaternized carbon dots with enhanced biofilm penetration and eradication efficiencies, J. Mater. Chem. B 7 (2019) 5104–5114, https://doi.org/10.1039/C9TB00681H.

[14] V. Zarghami, M. Ghorbani, K.P. Bagheri, M.A. Shokrgozar, Prevention the formation of biofilm on orthopedic implants by melittin thin layer on chitosan/bioactive glass/vancomycin coatings, J. Mater. Sci. Mater. Med. 32 (2021) 75, https://doi.org/10.1007/s10856-021-06551-5.

[15] A. Jose, M. Gizdavic-Nikolaidis, S. Swift, Antimicrobial coatings: reviewing options for healthcare applications, Appl. Microbiol. 3 (2023) 145–174, https://doi.org/10.3390/applmicrobiol3010012.

[16] S. Javaid, A. Mahmood, H. Nasir, M. Iqbal, N. Ahmed, N.M. Ahmad, Layer-by-layer self-assembled dip coating for antifouling functionalized finishing of cotton textile, Polymers 14 (2022) 2540, https://doi.org/10.3390/polym14132540.

[17] A.B. Asha, A. Ounkaew, Y.-Y. Peng, M. Gholipour, K. Ishihara, Y. Liu, R. Narain, Bioinspired antifouling and antibacterial polymer coating with intrinsic self-healing property, Biomater. Sci. (2022), https://doi.org/10.1039/d2bm01055k.

[18] G. Li, K. Lv, Q. Cheng, H. Xing, W. Xue, W. Zhang, Q. Lin, D. Ma, Enhanced bacterial-infected wound healing by nitric oxide-releasing topological supramolecular nanocarriers with self-optimized cooperative multi-point anchoring, Adv. Sci. 10 (2023) 2206959, https://doi.org/10.1002/advs.202206959.

[19] K. Suga, M. Murakami, S. Nakayama, K. Watanabe, S. Yamada, T. Tsuji, D. Nagao, Surface characteristics of antibacterial polystyrene nanoparticles synthesized using cationic initiator and comonomers, ACS Appl. Bio Mater. 5 (2022) 2202–2211, https://doi.org/10.1021/acsabm.2c00046.

[20] J. Wang, Y. Meng, Z. Jiang, M.T. Sarwar, L. Fu, H. Yang, Engineering nanoclay edges to enhance antimicrobial property against gram-negative bacteria: understanding the membrane destruction mechanism by contact-kill, Adv. Funct. Mater. 33 (2023) 2210406, https://doi.org/10.1002/adfm.202210406.

[21] A. Büter, G. Maschkowitz, M. Baum, Y.K. Mishra, L. Siebert, R. Adelung, H. Fickenscher, Antibacterial activity of nanostructured zinc oxide tetrapods, Int. J. Mol. Sci. 24 (2023) 3444, https://doi.org/10.3390/ijms24043444.

[22] G. Wang, C. Yang, M. Shan, H. Jia, S. Zhang, X. Chen, W. Liu, X. Liu, J. Chen, X. Wang, Synergistic poly(lactic acid) antibacterial surface combining superhydrophobicity for antiadhesion and chlorophyll for photodynamic therapy, Langmuir 38 (2022) 8987–8998, https://doi.org/10.1021/acs.langmuir.2c01377.

[23] X. Xu, Q. Wang, Y. Chang, Y. Zhang, H. Peng, A.K. Whittaker, C. Fu, Antifouling and antibacterial surfaces grafted with sulfur-containing copolymers, ACS Appl. Mater. Interfaces 14 (2022) 41400–41411, https://doi.org/10.1021/acsami.2c09698.

[24] A.B. Asha, Y.-Y. Peng, Q. Cheng, K. Ishihara, Y. Liu, R. Narain, Dopamine assisted self-cleaning, antifouling, and antibacterial coating via dynamic covalent interactions, ACS Appl. Mater. Interfaces 14 (2022) 9557–9569, https://doi.org/10.1021/acsami.1c19337.

[25] V. Carniello, B.W. Peterson, H.C. van der Mei, H.J. Busscher, Physico-chemistry from initial bacterial adhesion to surface-programmed biofilm growth, Adv. Colloid Interface Sci. 261 (2018) 1–14, https://doi.org/10.1016/j.cis.2018.10.005.

[26] H.-W. Chien, X.-Y. Chen, W.-P. Tsai, M. Lee, Inhibition of biofilm formation by rough shark skin-patterned surfaces, Colloids Surf. B Biointerfaces 186 (2020) 110738, https://doi.org/10.1016/j.colsurfb.2019.110738.

[27] S. Zheng, M. Bawazir, A. Dhall, H.-E. Kim, L. He, J. Heo, G. Hwang, Implication of surface properties, bacterial motility, and hydrodynamic conditions on bacterial surface sensing and their initial adhesion, Front. Bioeng. Biotechnol. 9 (2021) 643722, https://doi.org/10.3389/fbioe.2021.643722.

[28] O. Habimana, K. Steenkeste, M.-P. Fontaine-Aupart, M.-N. Bellon-Fontaine, S. Kulakauskas, R. Briandet, Diffusion of nanoparticles in biofilms is altered by bacterial cell wall hydrophobicity, Appl. Environ. Microbiol. 77 (2011) 367–368, https://doi.org/10.1128/AEM.02163-10.

[29] K. Ikuma, A.W. Decho, B.L.T. Lau, When nanoparticles meet biofilms—interactions guiding the environmental fate and accumulation of nanoparticles, Front. Microbiol. 6 (2015) 591, https://doi.org/10.3389/fmicb.2015.00591.

[30] S. Mallick, M. Nag, D. Lahiri, S. Pandit, T. Sarkar, S. Pati, N.P. Nirmal, H.A. Edinur, Z.A. Kari, M.R. Ahmad Mohd Zain, R.R. Ray, Engineered nanotechnology: an effective therapeutic platform for the chronic cutaneous wound, Nanomaterials 12 (2022) 778, https://doi.org/10.3390/nano12050778.

[31] H.H. Tuson, D.B. Weibel, Bacteria-surface interactions, Soft Matter 9 (2013) 4368–4380, https://doi.org/10.1039/C3SM27705D.

[32] S. Kreve, A.C.D. Reis, Bacterial adhesion to biomaterials: what regulates this attachment? A review, Jpn. Dent. Sci. Rev. 57 (2021) 85–96, https://doi.org/10.1016/j.jdsr.2021.05.003.

[33] S.P.S.N.B.S. Kumara, S.W.M.A.I. Senevirathne, A. Mathew, L. Bray, M. Mirkhalaf, P.K.D.V. Yarlagadda, Progress in nanostructured mechano-bactericidal polymeric surfaces for biomedical applications, Nanomaterials 13 (2023) 2799, https://doi.org/10.3390/nano13202799.

[34] S.K. Lower, R. Yongsunthon, N.N. Casillas-Ituarte, E.S. Taylor, A.C. DiBartola, B.H. Lower, T.J. Beveridge, A.W. Buck, V.G. Fowler, A tactile response in Staphylococcus aureus, Biophys. J. 99 (2010) 2803–2811, https://doi.org/10.1016/j.bpj.2010.08.063.

[35] N.C.T. Dadi, J. Bujdák, V. Medvecká, H. Pálková, M. Barlog, H. Bujdáková, Surface characterization and anti-biofilm effectiveness of hybrid films of polyurethane functionalized with saponite and phloxine B, Materials 14 (2021) 7583, https://doi.org/10.3390/ma14247583.

[36] E. Skoura, P. Boháč, M. Barlog, H. Pálková, A. Mautner, L. Bugyna, H. Bujdáková, J. Bujdák, Structure, photoactivity, and antimicrobial properties of phloxine B/poly(caprolactone) nanocomposite thin films, Appl. Clay Sci. 242 (2023) 107037, https://doi.org/10.1016/j.clay.2023.107037.

[37] A.R.L. Caires, T.H.N. Lima, T.F. Abelha, Conjugated polymer nanoparticles with tunable antibacterial photodynamic capability, Mater. Adv. 4 (2023) 1664–1670, https://doi.org/10.1039/D2MA00970F.

[38] C. Kromer, K. Schwibbert, S. Radunz, D. Thiele, P. Laux, A. Luch, H.R. Tschiche, ROS generating BODIPY loaded nanoparticles for photodynamic eradication of biofilms, Front. Microbiol. 14 (2023) 1274715, https://doi.org/10.3389/fmicb.2023.1274715.

[39] L. Sun, W. Jiang, H. Zhang, Y. Guo, W. Chen, Y. Jin, H. Chen, K. Du, H. Dai, J. Ji, B. Wang, Photosensitizer-Loaded multifunctional chitosan nanoparticles for simultaneous in situ imaging, highly efficient bacterial biofilm eradication, and tumor ablation, ACS Appl. Mater. Interfaces 11 (2019) 2302–2316, https://doi.org/10.1021/acsami.8b19522.

[40] W.-S. Kuo, P.-C. Wu, C.-Y. Hung, C.-Y. Chang, J.-Y. Wang, P.-C. Chen, M.-H. Hsieh, S.-H. Lin, C.-C. Chang, Y.-S. Lin, Nitrogen functionalities of amino-functionalized nitrogen-doped graphene quantum dots for highly efficient enhancement of antimicrobial therapy to eliminate methicillin-resistant Staphylococcus aureus and utilization as a contrast agent, Int. J. Mol. Sci. 22 (2021) 9695, https://doi.org/10.3390/ijms22189695.

[41] N.D. Hai, N. Huy, N.T.H. Nam, H. An, C.Q. Cong, N.M. Dat, L.M. Huong, L.T. Tai, N.H. Vu, N.T.N. Truong, N.H. Hieu, Comparative investigation of the characterization and photoactivity of gold-decorated graphitic carbon nitride: a study aspect of various synthesis approaches, Surf. Interfaces 44 (2024) 103645, https://doi.org/10.1016/j.surfin.2023.103645.

[42] N.C.T. Dadi, M. Dohál, V. Medvecká, J. Bujdák, K. Koči, A. Zahoranová, H. Bujdáková, Physico-chemical characterization and antimicrobial properties of hybrid film based on saponite and phloxine B, Molecules 26 (2021) 325, https://doi.org/10.3390/molecules26020325.

[43] S. Gnanasekar, G. Kasi, X. He, K. Zhang, L. Xu, E.-T. Kang, Recent advances in engineered polymeric materials for efficient photodynamic inactivation of bacterial pathogens, Bioact. Mater. 21 (2023) 157–174, https://doi.org/10.1016/j.bioactmat.2022.08.011.

[44] Y. Ren, H. Liu, X. Liu, Y. Zheng, Z. Li, C. Li, K.W.K. Yeung, S. Zhu, Y. Liang, Z. Cui, S. Wu, Photoresponsive materials for antibacterial applications, cell rep, Phys. Sci. 1 (2020) 100245, https://doi.org/10.1016/j.xcrp.2020.100245.

[45] A. Braoios, A. Pizzolitto, A. Fluminhan, Multiplex PCR use for Staphylococcus aureus identification and oxacillin and mupirocin resistance evaluation, Rev. Ciênc. Farm. Básica E Apl. 30 (2009) 303–307.

[46] European Committee On Antimicrobial Susceptibility Testing (EUCAST, version 13.0, 2023) Clinical breakpoints – breakpoints 682 and guidance. Available online: https://www.eucast.org/fileadmin/src/media/PDFs/EUCAST_files/Breakpoint_tables/v_13.0_Breakpoint_Tables.pdf (accessed on 10 November 2023), (n.d.).

[47] CLSI, M100 Performance Standards for Antimicrobial Susceptibility Testing, 28 Ed. CLSI Standards, Clinical and Laboratory Standards Institute, 2018.

[48] J.H. Merritt, D.E. Kadouri, G.A. O'Toole, Growing and analyzing static biofilms, Curr. Protoc. Microbiol 1 (2005), https://doi.org/10.1002/9780471729259.mc01b01s00. Unit-1B.1.

[49] B. Gaálová-Radochová, S. Kendra, L. Jordão, L. Kursawe, J. Kikhney, A. Moter, H. Bujdáková, Effect of quorum sensing molecule farnesol on mixed biofilms of Candida albicans and Staphylococcus aureus, Antibiotics 12 (2023) 441, https://doi.org/10.3390/antibiotics12030441.

[50] S. Stepanović, D. Vuković, V. Hola, G.D. Bonaventura, S. Djukić, I. Ćirković, F. Ruzicka, Quantification of biofilm in microtiter plates: overview of testing conditions and practical recommendations for assessment of biofilm production by staphylococci, APMIS 115 (2007) 891–899, https://doi.org/10.1111/j.1600-0463.2007.apm_630.x.

[51] T.D.L. Kaiser, E.M. Pereira, K.R.N. Dos Santos, E.L.N. Maciel, R.P. Schuenck, A.P.F. Nunes, Modification of the Congo red agar method to detect biofilm production by Staphylococcus epidermidis, Diagn. Microbiol. Infect. Dis. 75 (2013) 235–239, https://doi.org/10.1016/j.diagmicrobio.2012.11.014.

[52] K.J. Livak, T.D. Schmittgen, Analysis of relative gene expression data using real-time quantitative PCR and the $2-\Delta\Delta CT$ method, Methods 25 (2001) 402–408, https://doi.org/10.1006/meth.2001.1262.

[53] T. Theis, R.A. Skurray, M.H. Brown, Identification of suitable internal controls to study expression of a Staphylococcus aureus multidrug resistance system by quantitative real-time PCR, J. Microbiol. Methods 70 (2007) 355–362, https://doi.org/10.1016/j.mimet.2007.05.011.

[54] F. Shang, L. Li, L. Yu, J. Ni, X. Chen, T. Xue, Effects of stigmata maydis on the methicillin resistant *Staphylococus aureus* biofilm formation, PeerJ 7 (2019) e6461, https://doi.org/10.7717/peerj.6461.

[55] E.F. Kong, C. Tsui, S. Kucharíková, P. Van Dijck, M.A. Jabra-Rizk, Modulation of Staphylococcus aureus response to antimicrobials by the Candida albicans quorum sensing molecule farnesol, Antimicrob. Agents Chemother. 61 (2017), https://doi.org/10.1128/AAC.01573-17.

[56] H. Bujdáková, V. Bujdáková, H. Májeková-Koščová, B. Gaálová, V. Bizovská, P. Boháč, J. Bujdák, Antimicrobial activity of organoclays based on quaternary alkylammonium and alkylphosphonium surfactants and montmorillonite, Appl. Clay Sci. 158 (2018) 21–28, https://doi.org/10.1016/j.clay.2018.03.010.

[57] M. Alseqely, M. Newton-Foot, A. Khalil, M. El-Nakeeb, A. Whitelaw, A. Abouelfetouh, Association between fluoroquinolone resistance and MRSA genotype in Alexandria, Egypt, Sci. Rep. 11 (2021) 4253, https://doi.org/10.1038/s41598-021-83578-2.

[58] S.G. Weber, H.S. Gold, D.C. Hooper, A.W. Karchmer, Y. Carmeli, Fluoroquinolones and the risk for methicillin-resistant Staphylococcus aureus in hospitalized Patients 1, Emerg. Infect. Dis. 9 (2003) 1415–1422, https://doi.org/10.3201/eid0911.030284.

[59] C. Echeverria, M.D.T. Torres, M. Fernández-García, C. de la Fuente-Nunez, A. Muñoz-Bonilla, Physical methods for controlling bacterial colonization on polymer surfaces, Biotechnol. Adv. 43 (2020) 107586, https://doi.org/10.1016/j.biotechadv.2020.107586.

[60] Y. Qu, X. Zhu, R. Kong, K. Lu, T. Fan, Q. Yu, G. Wang, Dual-functional antibacterial hybrid film with antifouling and NIR-activated bactericidal properties, Compos. Part B Eng. 244 (2022) 110143, https://doi.org/10.1016/j.compositesb.2022.110143.

[61] H. Wang, L. Song, R. Jiang, Y. Fan, J. Zhao, L. Ren, Super-repellent photodynamic bactericidal hybrid membrane, J. Membr. Sci. 614 (2020) 118482, https://doi.org/10.1016/j.memsci.2020.118482.

[62] N. Pourmehdi, Z. Moradi-Shoeili, A. Sadat Naeemi, A. Salehzadeh, Biosynthesis of NiFe $_2$ O $_4$ @Ag nanocomposite and assessment of its effect on expression of *norA* gene in *Staphylococcus aureus*, Chem. Biodivers. 17 (2020) e2000072, https://doi.org/10.1002/cbdv.202000072.

[63] R.A. Prates, I.T. Kato, M.S. Ribeiro, G.P. Tegos, M.R. Hamblin, Influence of multidrug efflux systems on methylene blue-mediated photodynamic inactivation of Candida albicans, J. Antimicrob. Chemother. 66 (2011) 1525–1532, https://doi.org/10.1093/jac/dkr160.

[64] M.R. Hamblin, Chapter 8 - drug efflux pumps in photodynamic therapy, in: A. Sosnik, R. Bendayan (Eds.), Drug Efflux Pumps Cancer Resist. Pathw. Mol. Recognit. Charact. Possible Inhib. Strateg. Chemother., Academic Press, 2020, pp. 251–276, https://doi.org/10.1016/B978-0-12-816434-1.00008-5.

[65] J.P. O'Gara, Ica and beyond: biofilm mechanisms and regulation in Staphylococcus epidermidis and Staphylococcus aureus, FEMS Microbiol. Lett. 270 (2007) 179–188, https://doi.org/10.1111/j.1574-6968.2007.00688.x.

[66] Q. Peng, X. Tang, W. Dong, N. Sun, W. Yuan, A review of biofilm formation of Staphylococcus aureus and its regulation mechanism, Antibiotics 12 (2023), https://doi.org/10.3390/antibiotics12010012.

[67] G. Pietrocola, D. Campoccia, C. Motta, L. Montanaro, C.R. Arciola, P. Speziale, Colonization and infection of indwelling medical devices by Staphylococcus aureus with an emphasis on orthopedic implants, Int. J. Mol. Sci. 23 (2022) 5958, https://doi.org/10.3390/ijms23115958.

[68] C. Vuong, S. Kocianova, J.M. Voyich, Y. Yao, E.R. Fischer, F.R. DeLeo, M. Otto, A crucial role for exopolysaccharide modification in bacterial biofilm formation, immune evasion, and virulence, J. Biol. Chem. 279 (2004) 54881–54886, https://doi.org/10.1074/jbc.M411374200.

[69] H. Qi, H. Takano, Y. Kato, Q. Wu, C. Ogata, B. Zhu, Y. Murata, Y. Nakamura, Hydogen peroxide-dependent photocytotoxicity by phloxine B, a xanthene-type food colorant, Biochim. Biophys. Acta BBA - Gen. Subj. 1810 (2011) 704–712, https://doi.org/10.1016/j.bbagen.2011.04.010.

[70] M.P. Murphy, H. Bayir, V. Belousov, C.J. Chang, K.J.A. Davies, M.J. Davies, T.P. Dick, T. Finkel, H.J. Forman, Y. Janssen-Heininger, D. Gems, V.E. Kagan, B. Kalyanaraman, N.-G. Larsson, G.L. Milne, T. Nyström, H.E. Poulsen, R. Radi, H. Van Remmen, P.T. Schumacker, P.J. Thornalley, S. Toyokuni, C. C. Winterbourn, H. Yin, B. Halliwell, Guidelines for measuring reactive oxygen species and oxidative damage in cells and in vivo, Nat. Metab. 4 (2022) 651–662, https://doi.org/10.1038/s42255-022-00591-z.